Freeze-dried chitosan-platelet-rich plasma implants for rotator cuff tear repair: Pilot ovine studies

Gabrielle Deprés-Tremblay BSc [1], Anik Chevrier PhD [2], Mark B Hurtig DVM [3], Martyn Snow MD [4], Scott Rodeo MD [5] and Michael D Buschmann PhD [1,2]

[1]Biomedical Engineering Institute and [2]Chemical Engineering Department, Polytechnique, Montreal, QC, Canada, [3]Department of Clinical Studies, University of Guelph, Guelph, ON, Canada, [4]The Royal Orthopaedic Hospital, Birmingham, UK, [5]Sports Medicine and Shoulder Service, The Hospital for Special Surgery, New York, NY, USA

Running title: Chitosan-PRP for rotator cuff repair in ovine models

Corresponding author: Prof Michael D. Buschmann, Biomedical Engineering Institute and Chemical Engineering Department, Polytechnique Montreal, PO Box 6079 Succ Centre-Ville, Montreal, Quebec, Canada, H3C 3A7, Fax: 514 340 2980 Tel: 514 340 4711 ext. 4931, E-mail: michael.buschmann@polymtl.ca

Abstract

Rotator cuff tear is one of the most common sources of shoulder pathology. Different suturing techniques have been used for surgical cuff repair, but re-tears remain a significant clinical challenge. The objective of this study was to investigate the effect of using chitosan (CS)-platelet-rich plasma (PRP) implants in conjunction with suture anchors in chronic and acute ovine rotator cuff tear models. In two subsequent pilot feasibility studies, unilateral full-thickness tears were created in the infraspinatus (ISP) tendon of mature female Texel-Cross sheep. In the chronic model (n=4 sheep), the tendons were capped with silicon and allowed to degenerate to chronic stage for 6 weeks, while the tendons were immediately repaired in the acute model (n=4 sheep). Transected ISP tendons were reattached with suture anchors and, in the case of treated shoulders, implants composed of freeze-dried CS solubilized in autologous PRP were additionally applied to the tendon-bone interface and on top of the repaired site. The chronic defect model induced significant tendon degeneration and retraction, which made repair more challenging than in the acute defect model. Treatment with CS-PRP implants induced recruitment of polymorphonuclear cells at 2 weeks post-operative and improved ISP tendon structural organization at 3 months. Treatment also increased bone remodeling and ingrowth at the tendon-bone interface at 3 months, suggesting that a more robust attachment could be achieved by combining CS-PRP implants with suture anchors. These pilot studies provide the first evidence that CS-PRP implants can improve rotator cuff repair in large animal models.

Keywords

Rotator cuff tears, chitosan, platelet-rich plasma, chronic repair, acute repair, ovine models

Introduction

Rotator cuff tears are a common cause of morbidity in adults and one of the most common shoulder pathologies (Lehman et al., 1995; Lippi et al., 2010). Cuff tears are associated with fatty infiltration, muscle atrophy (Goutallier et al., 1994; Thomazeau et al., 1997), tendon retraction, and structural and architectural alterations of the musculotendinous unit (Patte 1990). Ruptures of rotator cuff tendons may eventually lead to irreversible changes in the shoulder, causing intolerable chronic pain and severe functional disability. Persistent tendon defects with constant exposure of the intra-articular joint surface and fluid will occur if a rotator cuff tear is not repaired within a certain time-frame after injury (Derwin et al., 2007). It is believed that there may be a "point of no return" in rotator cuff injury, with formation of scar tissue and infiltration of fat, after which the elasticity of the muscle-tendon unit can no longer return to normal (Laron et al., 2012).

Different suturing techniques have been used for tendon fixation in cuff repair. The goal of using suture anchors is to restore the initial footprint by suturing the tendon directly to the tuberosity, while increasing initial fixation strength, and mechanical stability under cyclic loading (Cole et al., 2007). These procedures are assumed to increase footprint contact area, and restore normal structure and function of the shoulder (Giovanni Di Giacomo 2008), while improving the rate of healing (Denard and Burkhart 2013). However, patients often experience re-tears (Harryman et al., 1991; Galatz et al., 2004). Failure to heal occurs in 20 to 95% of cases at 2-years following surgical repair (Harryman et al., 1991; Gazielly et al., 1994; Yamaguchi et al., 2001; Bey et al., 2002; Adams et al., 2006; Brennan et al., 2006; Brown et al., 2009), depending on surgical treatment used (Iannotti et al., 1994; Meyer et al., 2004), time from injury (Bartolozzi et al., 1994), tendon quality (Riley et al., 1994), muscle quality (Goutallier et al.,

2003), biological healing response (Hamada et al., 1997), patient age, number of tendons involved, and tear size (Barber et al., 2011). One limitation of current surgical procedures is that regeneration of the enthesis is not achieved following surgical fixation, and augmentation techniques could possibly overcome this limitation (Deprés-Tremblay et al., 2016).

Growth factors are known to be important in cell chemotaxis, proliferation, matrix synthesis and cell differentiation (Gulotta and Rodeo 2009), and platelet-rich plasma (PRP) is a readily available source of autologous growth factors. PRP injections have been used clinically to treat rotator cuff tears, since it is believed that increased concentration of platelet-derived growth factors will stimulate revascularization of soft tissue and enhance tendon healing (Barber et al., 2011). However, current clinical evidence does not support the routine use of PRP injections to treat rotator cuff tears (Chahal et al., 2012; Li et al., 2014; Vavken et al., 2015; Warth et al., 2015; Zhao et al., 2015) and PRP injections are still very controversial in the orthopaedic field. Variability in the isolation protocols and resulting preparations and the poor stability of PRP *in vivo* are two possible reasons why results have been inconsistent to date.

Chitosan (CS) is a biodegradable polymer that has been used for several tissue repair and regeneration applications. Our laboratory has implemented the use of PRP combined with freeze-dried CS to form injectable implants that coagulate *in situ* (Chevrier et al., 2017). *In vitro* release of platelet-derived growth factors is increased and platelet-mediated clot retraction is inhibited by mixing PRP with chitosan (Deprés-Tremblay et al., 2016). CS-PRP implants were shown to reside for at least 6 weeks subcutaneously *in vivo* and enhance cell recruitment to surrounding tissues compared to PRP alone (Deprés-Tremblay et al., 2016; Chevrier et al., 2017). CS-PRP implants were tested in ovine meniscus repair models where they increased cell recruitment, vascularization, remodelling and repair tissue integration compared to injection of PRP alone or

wrapping the meniscus with a collagen membrane (Chevrier et al., 2016; Ghazi zadeh et al., 2017). Finally, CS-PRP implants improved marrow-stimulated cartilage repair and induced bone remodeling in a chronic rabbit defect model (Dwivedi et al., 2017). We hypothesized that all of the above would also be beneficial to rotator cuff repair, and we subsequently showed in a small rabbit model that CS-PRP implants improve transosseous rotator cuff repair, by favoring tendon attachment through increased bone remodeling (Deprés-Tremblay et al., 2017).

The two pilot feasibility studies presented here investigated whether CS-PRP implants can also improve rotator cuff repair in larger sheep models. The first study used a chronic repair model, where tendons were allowed to degenerate to a chronic stage prior to repair, while an acute model with immediate repair was used in the second study. In both repair models, the infraspinatus (ISP) tendons were surgically transected and repaired using suture anchors with or without additional application of CS-PRP implants and healing was assessed histologically. Our starting hypothesis was that CS-PRP implants would have positive effects on chronic and acute rotator cuff repair through increased cell recruitment, vascularization and bone remodelling.

Materials and methods

Preparation of freeze-dried chitosan formulations

Chitosan (degree of deacetylation 80.2%, number average molar mass M_n 36,000 g/mol, weight average molar mass M_w 65,000 g/mol, polydispersity index 1.8) was used to prepare formulations containing 1% (w/v) chitosan, 28 mM HCl, 1% (w/v) trehalose as a lyoprotecting agent (Life Science) and 42.2 mM $CaCl_2$ as a PRP activator (Sigma-Aldrich). Formulations were filter-sterilized and distributed in 1 mL aliquots into sterile, de-pyrogenized 3cc glass vials for lyophilization using the following steps: 1) ramped freezing to -40^{o}C in 1 hour, isothermal 2

hours at -40^{o}C, 2) -40^{o}C for 48 hours, 3) ramped heating to 30^{o}C in 12 hours, isothermal 6 hours at 30^{o}C, at 100 millitorrs.

Preparation of platelet-rich plasma (PRP)

Blood was drawn from the sheep jugular immediately prior to surgery. One small tube of blood was drawn for complete blood count and platelet analysis. Then, two tubes of 9 mL blood were collected per sheep and anti-coagulated with 1 mL 3.8% (w/v) sodium citrate each (final citrate concentration 12.9 mM). Blood was centrifuged for 10 min at 1300 rpm and then for 10 min at 2000 rpm using the ACE EZ-PRP centrifuge to extract ~ 3 mL PRP per sheep. The isolated PRP contained an average of 409 X 10E9/L platelets, 6.2 X 10E9/L leukocytes and 2.4 X 10E12/L erythrocytes.

Experimental study design and surgical technique

The protocol for this study was approved by the University of Montreal committee "Comité de déontologie de l'expérimentation sur les animaux" (initial date of approval March 10th 2016) and was consistent with the Canadian Council on Animal Care guidelines for the care and use of laboratory animals. Eight adult Texel-Cross female sheep (age ranging from 2-6 years; weight ranging from 55-70kg) were divided into a chronic repair model group (**Table 1**) and an acute repair model group (**Table 2**). In both groups, the surgical method included unilateral exposure of the infraspinatus tendons (ISP) through a muscle separating approach to the lateral aspect of the shoulder using general anesthesia and aseptic technique. The ISP tendon was transected from its original footprint on the humerus, creating a full-thickness rotator cuff tear. The humeral head was debrided with a surgical scalpel removing any tendinous tissue still

attached. In both the chronic and acute repair models, the surface of the tuberosity was roughened with use of a curet and the tendon surface slightly abraded prior to anchor insertion.

In the chronic repair model (**Table 1 & Figure 1**), the tendons were capped with a 5-cm silicon tube to prevent spontaneous repair and allow the tear to degenerate to a chronic stage for 6 weeks. The capped tendons were engulfed in scar tissue after 6 weeks, at the time of the second surgery. After freeing the tendons from scar tissue and removing the silicon tubes, we found that the muscle-tendon unit had significantly retracted, leaving a gap of several centimeters between the end of the tendon and the tuberosity. In two sheep, the ISP tendons were torn as soon as they were pulled to close the gap to the tuberosity, and were found to be unrepairable. Therefore, in those 2 sheep, a defect was created in the contralateral shoulders, but this time the ISP tendon was capped with a shorter 5-mm silicon tube and allowed to degenerate to a chronic stage for 2 weeks. In the third sheep, the 6-week chronic defect was repaired with suture anchors and sutured in a suture bridge configuration using four 4.65 mm PEEK Swivelock anchors and 2 mm FiberTape sutures (Arthrex, Product N^{o} AR2324-PSLC and AR-7237). In the fourth sheep, the 6-week chronic defect was repaired with one suture anchor with the ISP tendon sutured using a Masson-Allen configuration and the CS-PRP implant was additionally applied in a 2-part manner. Freeze-dried chitosan (1mL cake) was solubilized with 1 mL autologous PRP and 0.5 mL CS-PRP injected at the footprint prior to anchor insertion and then 0.5 mL CS-PRP was injected on top and under the tendon after reattachment. In both of the above repairable cases, the tendons were too retracted to be reattached at the footprint, hence a gap remained between the tendon and tuberosity after repair. The animals were allowed to walk ad libitum postoperatively and necropsy was 2 weeks after second surgery (n=4 sheep).

In the acute repair model (**Table 2 & Figure 2**), the tendons were transected and immediately repaired with suture anchors and sutured in a suture bridge configuration using four 4.65 mm PEEK Swivelock anchors and 2 mm FiberTape sutures (Arthrex, Product N^{o} AR2324-PSLC and AR-7237). In the treated shoulders, CS-PRP implants were additionally applied in a 2-part manner. The first row of anchors was securely inserted and the sutures were passed through the ISP tendon. Freeze-dried chitosan (1mL cake) was solubilized with 1 mL autologous PRP and 0.5 mL CS-PRP was injected at the footprint. The sutures were tightened and the second row of anchors was inserted. Then, 0.5 mL CS-PRP was injected on top of the repaired site and under the tendon. The animals were allowed to walk ad libitum postoperatively and necropsy was 6 weeks (n=2 sheep) and 3 months (n=2 sheep) after repair.

Specimen collection and histological processing

Animals were euthanized by sedation followed by captive bolt pistol. The shoulders were dissected and the humeral head-ISP-tendon unit complex was harvested en bloc from just proximal to the musculotendinous junction. Glenoid surfaces, muscle biopsies and synovial membrane biopsies were collected. All samples were fixed for several days in 10% neutral buffered formalin and trimmed for further processing. The ISP insertion sites, humeral head and glenoid surfaces were decalcified with HCl with trace glutaraldehyde. All samples were dehydrated in graded ethanol series, cleared with xylene and embedded in paraffin. Sections (5µm thickness) were stained with Safranin O/Fast Green or Hematoxylin and Eosin, scanned with a Nanozoomer RS (Hamamatsu) and images exported using NDP View software (Hamamatsu) for qualitative histological assessment. In addition, polarized microscopy images

of the ISP tendons were obtained with an Axiolab (Zeiss) microscope equipped with a CCD camera (Hitachi HV-F22 Progressive Scan Colour 3-CCD).

Results

The chronic repair model was more challenging than the acute repair model

After 6 weeks of chronic degeneration, ISP tendons capped with 5-cm silicon tubes became macroscopically abnormal throughout and were red, spongy (**Figure 1d**), biomechanically weak, easily torn with 2 tendons out of 4 unrepairable. Significant retraction had occurred so that the 2 of 4 tendons that could be repaired could not be reattached at their original footprint. In the two cases where the tendons were found to be unrepairable, a decision was made to operate on the contralateral shoulders, cap the ISP tendons with smaller 5-mm silicon tubes and allow the tears to degenerate to a chronic stage for 2 weeks. Significant retraction and structural abnormalities of the ISP tendon under the capped end were apparent after 2 weeks (**Figure 1f**), although changes were less severe than in the 6-week chronic model. In both the 6-week capped and the 2-week capped unrepaired defects, abundant scar tissue was engulfing the capped ISP tendons and bridging the gap to the tuberosity, which suggests that a robust repair response occurs in this model, even in the presence of a silicon barrier. In contrast to the chronic model, the acute tear model was easily executed and the transected ISP tendons could be reattached at the footprint (**Figure 2**).

CS-PRP implants induced recruitment of polymorphonuclear cells to the ISP tendon at 2 weeks and improved ISP tendon structural organization at 3 months

As expected, intact ISP tendons consisted of fibrocartilaginous tissue organized in bundles with sparse cells and a small amount of glycosaminoglycans (GAG) (**Figure 3a-c & Figure 4a-d**). Histologically, none of the test tendons were structurally similar to intact (**Figures 3 & 4**). Acellular areas were observed in ISP tendons of the chronic defect model, for both the 2-week capped and the 6-week capped, (**Figure 3**), but not in tendons of the acute model (**Figure 4**). The 6-week chronic defect repaired with anchors + CS-PRP for 2 weeks had a portion of tendon repair tissue that was rich in polymorphonuclear cells (**Figure 3o**). In the acute model, treatment with anchors induced chondrogenesis within the tendon body at 6 weeks (**Figure 4f**) and abundant GAG expression at 3 months (**Figure 4m**), while this was not observed in the case of treatment with anchors + CS-PRP (**Figures 4 i & q**). Repaired tendons consisted mainly of disorganized, hypercellular and vascularized tissues (**Figures 3 & 4**). The one exception was the tendon treated with anchors + CS-PRP at 3 months in the acute model, which was mostly organized in bundles and had a portion of repair tissue that was structurally similar to normal tendon (**Figure 4q-t**). Polarized light microscopy images better highlight the tendon structural organization, confirming the beneficial effect of treatment with anchors + CS-PRP in the acute model at 3 months (**Figure 4t**).

CS-PRP implants increased bone remodeling at the ISP tendon-bone junction

Histologically, none of the repaired insertions sites had structure identical to intact entheses, where for the latter, the tidemark was easily recognizable and no scar tissue was present above the bone front (**Figure 5a-c & Figure 6a-c**). The enthesis was still structurally normal in the 2-week capped chronic defects (**Figure 5d**), but not in any other group (**Figures 5 & 6**). In all cases, even in untreated chronic defects (**Figure 5 d & g**), scar tissue was growing

superior to the enthesis and integration of the scar tissue with the underlying bone was achieved through bone remodeling and ingrowth at the junction of the scar tissue with the original bone front (**Figures 5 & 6**). Treatment with anchors + CS-PRP increased bone remodeling and GAG expression at the tendon-bone junction in both the chronic repair model (**Figure 5m-o**) and the acute repair model (**Figure 6m-o**).

CS-PRP implants did not induce any treatment-specific deleterious effects in the shoulder joint

In both the chronic and acute repair models, the humeral head was macroscopically free of defects, while synovial fossas were apparent at the center of almost all of the glenoid surfaces. Almost all humeral heads, including intact controls, showed signs of GAG depletion (**Figure 7a, c, e, g & i**). Several glenoids, including intact controls, exhibited GAG depletion as well as other structural abnormalities including, hypercellularity, cell cloning and fissures (**Figure 7k-m**). Muscle histology showed increased fatty infiltration in chronic defects as early as 2 weeks after defect creation, which was not reversed by repair (**Figure 8 b & c**). Similarly, fatty infiltration was also induced by surgical detachment and immediate reattachment in the acute repair model (**Figure 8 d & e**). Histology of the synovial membranes showed that different forms of normal synovium can be found in sheep shoulders including the adipose form of synovium and the fibrous form of synovium (**Figure 9**). There was mild synovitis and increased cell infiltration in the chronic model treated with anchors + CS-PRP for 2 weeks (**Figure 9c**), but not in any other sample.

Discussion

The purpose of the current study was to determine whether CS-PRP implants can improve rotator cuff repair in chronic and acute repair models in the sheep. Large animal models, like sheep, have infraspinatus tendons that are similar in size to the human supraspinatus (Edelstein et al., 2011), making them amenable to using repair techniques commonly employed in humans (Derwin et al., 2007; Schlegel et al., 2007), as was done here with suture anchors. Our starting hypothesis was supported in that treatment with anchors + CS-PRP implants led to improved tendon structural appearance and increased bone remodeling and ingrowth at the tendon-bone junction.

One unexpected and important finding reported here, were the difficulties we faced during implementation of the chronic repair model. We found that capping the ISP tendons for 6 weeks with 5-cm silicon tubes likely prevented proper nutrient diffusion and led to cell death and severe tendon degeneration, which rendered some tendons unrepairable. Although degeneration was not as marked when the tendons were capped for 2 weeks with 5-mm silicon length, reattachment at the footprint would have been difficult to achieve since the tendon-muscle unit had significantly retracted. Capping with silicon has been used by other research groups studying chronic rotator cuff repair in sheep, but the surgery usually involves osteotomy, leaving a small bone chip attached to the ISP tendon, with the silicon covering the bone chip and not the tendon itself (Gerber et al., 2004; Meyer et al., 2004). Other groups have used a Preclude sheet to wrap the ISP tendon and allow the tears to develop to chronic stage (Coleman et al., 2003; Uggen et al., 2010). Preclude is a dura substitute composed of Gore-Tex, with pores of <1μm in size, which would still allow nutrient diffusion to the tendons, and most likely would have been a better choice than silicon in the current study. We found that abundant scar tissues were bridging the gap between the capped tendon and the tuberosity after 2 weeks and 6 weeks, which supports

the notion that the healing response is robust and spontaneous in sheep even in these chronic models (Gerber et al., 2004; Meyer et al., 2004). As of now, we consider the acute repair model to be more consistent and easily reproducible.

Even though this study presented some challenges, some interesting findings are worth further discussion. Polymorphonuclear (PMN) cells were observed in the tendon repair tissue of the shoulder treated with anchors + CS-PRP for 2 weeks, which is not unexpected at this time point, since CS-PRP implants were previously shown to induce PMN recruitment for at least 2 weeks in a rabbit transosseous rotator cuff repair model (Deprés-Tremblay et al., 2017). PMN recruitment was abrogated by 6 weeks, which suggests that CS-PRP implants were fully degraded by then, which is consistent with previous sheep studies using similar doses of the CS-PRP implants, albeit in the knee joint for meniscus repair (Chevrier et al., 2016; Ghazi zadeh et al., 2017). Similarly to what was previously seen in the transosseous rotator cuff repair model in the rabbit, the tendon treated with anchors only showed chondrogenesis and GAG expression within the tendon body at 6 weeks, while the tendon treated with anchors + CS-PRP did not. The significance of chondrogenesis occurring within the tendon repair tissue is still unclear, but we hypothesize that this may be the first step in heterotopic ossification, a well known complication of tendon injury, which we previously found was inhibited by treatment with CS-PRP implants in the transosseous rabbit model (Deprés-Tremblay et al., 2017). The anchors + CS-PRP repair technique resulted in better tendon structural outcome than anchors only at 3 months only with no apparent improvement at 6 weeks, possibly through a modulation of timing of the healing sequence or through increased repair tissue remodeling.

During development, tendon-bone integration occurs through establishment of an embryonic tendon-bone attachment unit, which matures into the fibrocartilaginous insertion,

known as the enthesis (Thomopoulos et al., 2010; Zelzer et al., 2014). Maturation of the enthesis appears to follow pathways similar to the growth plate development (Thomopoulos et al., 2010). The insertion site matures through mineralization of chondrocyte-like cells, with associated remodeling through osteoclasts and osteoblasts, creating the interface between tendon and the tuberosity (Thomopoulos et al., 2010). Following repair however, tendon-bone insertion usually heals through a fibrovascular scar tissue formation, lacking any sort of reestablishment of the four zones of the native enthesis (Apostolakos et al., 2014). Rotator cuff healing occurs in overlapping phases similar to those observed in the case of wound healing, namely the inflammatory phase, the matrix production phase and the remodeling phase (Galatz 2013). In the chronic and acute models used here, the integration of the tendon repair tissue occurred through bone remodeling and ingrowth at the junction between the tendon and the underlying bone, and the native structure of the enthesis was not re-established. Bone remodeling appears to be a mechanism that enables the repair to become mechanically stronger. It has previously been suggested that strong healing between tendon and the tuberosity, with reformation of a new enthesis, necessitates bone ingrowth into scar tissue and outer tendon (Sanchez Marquez et al., 2011). Other authors have suggested that the formation of a callus appears to be essential for remodelling the tendon-bone boundary after injury (Newsham-West et al., 2007). In that respect, it is significant that bone remodeling and GAG expression were greater in the case of the insertion sites treated with anchors + CS-PRP compared to suture anchors only, although it is impossible to draw solid conclusions on the basis of such a small number of samples. Of note, CS-PRP implants have previously been shown to increase bone remodeling over standard treatment in the context of rotator cuff and cartilage repair in small rabbit models, leading to better integration of repair tissues (Deprés-Tremblay et al., 2017; Dwivedi et al., 2017).

There were no treatment-specific deleterious effects in the shoulder joint, suggesting that CS-PRP implants have high safety. Structural abnormalities were visible in most glenoids, suggesting that greater stresses are applied on that surface compared to the humeral head in the sheep model. Fatty infiltration of the ISP muscle was induced in both chronic and acute models, and no treatment could reverse that effect. A longer follow-up time may be required to see treatment-specific protective effects. Mild transient synovitis was present in the shoulder treated with CS-PRP at 2 weeks, and this was resolved at the later 6 weeks and 3 month time points, once the biomaterial was degraded.

There were several limitations to this study. The main limitation is the small number of animals used, although we feel that these numbers were reasonable for pilot feasibility studies. Obviously, a larger number of animals would be required to draw firm conclusions, and the results reported here should be viewed with caution. Furthermore, although the sheep is a commonly used model of rotator cuff repair, it is not identical to human. In contrast to humans, the sheep infraspinatus tendon is not intraarticular, although a bursa exists underneath the tendon. The sheep forelimb is also weight-bearing, has no clavicle, a less-developed acromion, and no coracoacromial arch (Turner 2007). Most importantly, robust scar tissue formation occurs between tendon stump and the bone in the sheep, not analogous to humans, where gaping is a common recurrent problem. Finally, assessment was purely qualitative and, although improved histological appearance would be expected to translate into superior performance, no other type of measurement was performed.

In summary, developing techniques to augment of rotator cuff repair remains clinically relevant. The technical challenges associated with the chronic repair model in the sheep make the acute model preferable for future studies. Despite their limitations, these two pilot studies

provide the first evidence that CS-PRP implants improve the healing response in large animal models of rotator cuff repair, partly through increased bone remodeling at the tendon repair tissue and underlying bone interface. Future work will involve a larger number of animals and a longer duration of follow-up, with the long-term objective of translating this technology to the clinic.

Acknowledgments

We acknowledge the technical contributions of Geneviève Picard and the funding sources (Canadian Institutes of Health Research, Canada Foundation for Innovation, Groupe de Recherche en Sciences et Technologies Biomédicales, Natural Sciences and Engineering Research Council of Canada, Ortho Regenerative Technologies Inc).

Competing interest statement

AC, MBH and MDB hold shares, MDB is a Director of, and MS and SR are clinical advisors of Ortho Regenerative Technologies Inc.

References

Adams JE, Zobitz ME, Reach JS, An KN,Steinmann SP. 2006, Rotator Cuff Repair Using an Acellular Dermal Matrix Graft: An In Vivo Study in a Canine Model, *Arthroscopy,* **22**, 7: 700-709.

Apostolakos J, Durant TJ, Dwyer CR, Russell RP, Weinreb JH, Alaee F, Beitzel K, McCarthy MB, Cote MP,Mazzocca AD. 2014, The enthesis: a review of the tendon-to-bone insertion, *Muscles Ligaments Tendons J,* **4**, 3: 333-342.

Barber FA, Hrnack SA, Snyder SJ,Hapa O. 2011, Rotator Cuff Repair Healing Influenced by Platelet-Rich Plasma Construct Augmentation: A Novel Molecular Mechanism Reply, *Arthroscopy,* **27**, 11: 1456-1457.

Bartolozzi A, Andreychik D,Ahmad S. 1994, Determinants of outcome in the treatment of rotator cuff disease, *Clin Orthop Relat Res,* 308: 90-97.

Bey MJ, Song HK, Wehrli FW,Soslowsky LJ. 2002, A noncontact, nondestructive method for quantifying intratissue deformations and strains, *J Biomech Eng,* **124**, 2: 253-258.

Brennan EP, Reing J, Chew D, Myers-Irvin JM, Young EJ,Badylak SF. 2006, Antibacterial activity within degradation products of biological scaffolds composed of extracellular matrix, *Tissue Eng,* **12**, 10: 2949-2955.

Brown BN, Valentin JE, Stewart-Akers AM, McCabe GP,Badylak SF. 2009, Macrophage phenotype and remodeling outcomes in response to biologic scaffolds with and without a cellular component, *Biomaterials,* **30**, 8: 1482-1491.

Chahal J, Van Thiel GS, Mall N, Heard W, Bach BR, Cole BJ, Nicholson GP, Verma NN, Whelan DB,Romeo AA. 2012, The Role of Platelet-Rich Plasma in Arthroscopic Rotator Cuff Repair: A Systematic Review With Quantitative Synthesis, *Arthroscopy,* **28**, 11: 1718-1727.

Chevrier A, Darras V, Picard G, Nelea M, Veilleux D, Lavertu M, Hoemann CD,Buschmann MD. 2017, Injectable chitosan-platelet-rich plasma (PRP) implants to promote tissue regeneration: In vitro properties, in vivo residence, degradation, cell recruitment and vascularization, *J Tissue Eng Regen Med,*

Chevrier A, Deprés-Tremblay G, Hurtig MB,Buschmann MD (2016). Chitosan-platelet-rich plasma implants can be injected into meniscus defects to improve repair. Transactions Orthopaedic Research Society, Orlando, FL, USA.

Cole BJ, ElAttrache NS,Anbari A. 2007, Arthroscopic rotator cuff repairs: An anatomic and biomechanical rationale for different suture-anchor repair configurations, *Arthroscopy,* **23**, 6: 662-669.

Coleman SH, Fealy S, Ehteshami JR, MacGillivray JD, Altchek DW, Warren RF,Turner AS. 2003, Chronic rotator cuff injury and repair model in sheep, *Journal of Bone and Joint Surgery-American Volume,* **85A**, 12: 2391-2402.

Denard PJ,Burkhart SS. 2013, The Evolution of Suture Anchors in Arthroscopic Rotator Cuff Repair, *Arthroscopy,* **29**, 9: 1589-1595.

Deprés-Tremblay G, Chevrier A, Snow M, Hurtig MB, Rodeo S,Buschmann MD. 2016, Rotator cuff repair: a review of surgical techniques, animal models, and new technologies under development, *J Shoulder Elbow Surg,*

Deprés-Tremblay G, Chevrier A, Snow M, Rodeo S,Buschmann MD (2017). Freeze-dried chitosan-PRP in a rabbit model of rotator cuff repair. Trasactions Orthopaedic Research Society.

Deprés-Tremblay G, Chevrier A, Tran-Khanh N, Nelea M,Buschmann MD (2016). Chitosan-platelet-rich plasma implants for tissue repair - in vitro and in vivo characteristics. World Biomaterials Congress. Montreal, QC, Canada.

Derwin KA, Baker AR, Codsi MJ,Iannotti JP. 2007, Assessment of the canine model of rotator cuff injury and repair, *Journal of Shoulder and Elbow Surgery,* **16**, 5: 140S-148S.

Dwivedi G, Chevrier A, Hoemann CD,Buschmann MD (2017). Freeze dried chitosan/platelet-rich-plasma implants improve marrow stimulated cartilage repair in rabbit chronic defect model Transactions Orthopaedic Research Society. San Diego, CA, USA.

Edelstein L, Thomas SJ,Soslowsky LJ. 2011, Rotator Cuff Tears: What have we learned from animal models?, *Journal of Musculoskeletal & Neuronal Interactions,* **11**, 2: 150-162.

Galatz LM. 2013, 'Soft Tissue to Bone Healing in Rotator Cuff Repair'. *Structural Interfaces and Attachments in Biology*, Springer Science+Business Media, New York, NY, USA; Pages.

Galatz LM, Ball CM, Teefey SA, Middleton WD,Yamaguchi K. 2004, The outcome and repair integrity of completely arthroscopically repaired large and massive rotator cuff tears, *Journal of Bone and Joint Surgery-American Volume,* **86A**, 2: 219-224.

Gazielly DF, Gleyze P,Montagnon C. 1994, Functional and anatomical results after rotator cuff repair, *Clin Orthop Relat Res,* 304: 43-53.

Gerber C, Meyer DC, Schneeberger AG, Hoppeler H,Von Rechenberg B. 2004, Effect of tendon release and delayed repair on the structure of the muscles of the rotator cuff: An experimental study in sheep, *Journal of Bone and Joint Surgery-American Volume,* **86A**, 9: 1973-1982.

Ghazi zadeh L, Chevrier A, Hurtig MB, Farr J, Rodeo S, Hoemann CD,Buschmann MD (2017). Freeze-dried chitosan-PRP implants improve meniscus repair in an ovine model. Transactions Orthopaedic Research Society, San Diego, CA, USA.

Giovanni Di Giacomo NP, Alberto Costantini , Andrea De Vita (2008). Atlas of Functional Shoulder Anatomy. Rome, Italy, Springer.

Goutallier D, Postel JM, Bernageau J, Lavau L,Voisin MC. 1994, Fatty muscle degeneration in cuff ruptures. Pre- and postoperative evaluation by CT scan, *Clin Orthop Relat Res,* 304: 78-83.

Goutallier D, Postel JM, Gleyze P, Leguilloux P,Van Driessche S. 2003, Influence of cuff muscle fatty degeneration on anatomic and functional outcomes after simple suture of full-thickness tears, *J Shoulder Elbow Surg,* **12**, 6: 550-554.

Gulotta LV,Rodeo SA. 2009, Growth factors for rotator cuff repair, *Clin Sports Med,* **28**, 1: 13-23.

Hamada K, Tomonaga A, Gotoh M, Yamakawa H,Fukuda H. 1997, Intrinsic healing capacity and tearing process of torn supraspinatus tendons: in situ hybridization study of alpha 1 (I) procollagen mRNA, *J Orthop Res,* **15**, 1: 24-32.

Harryman DT, 2nd, Mack LA, Wang KY, Jackins SE, Richardson ML,Matsen FA, 3rd. 1991, Repairs of the rotator cuff. Correlation of functional results with integrity of the cuff, *J Bone Joint Surg Am,* **73**, 7: 982-989.

Iannotti JP, Williams GR,Patel NJ. 1994, Advances in the surgical treatment of disorders of the shoulder, *Surg Annu,* **26**, 227-250.

Laron D, Samagh SP, Liu X, Kim HT,Feeley BT. 2012, Muscle degeneration in rotator cuff tears, *Journal of Shoulder and Elbow Surgery,* **21**, 2: 164-174.

Lehman C, Cuomo F, Kummer FJ,Zuckerman JD. 1995, The incidence of full thickness rotator cuff tears in a large cadaveric population, *Bull Hosp Jt Dis,* **54**, 1: 30-31.

Li X, Xu C-P, Hou Y-L, Song J-Q, Cui Z,Yu B. 2014, Are Platelet Concentrates an Ideal Biomaterial for Arthroscopic Rotator Cuff Repair? A Meta-analysis of Randomized Controlled Trials, *Arthroscopy,* **30**, 11: 1483-1490.

Lippi G, Longo UG,Maffulli N. 2010, Genetics and sports, *Br Med Bull,* **93**, 27-47.

Meyer DC, Hoppeler H, von Rechenberg B,Gerber C. 2004, A pathomechanical concept explains muscle loss and fatty muscular changes following surgical tendon release, *Journal of Orthopaedic Research,* **22**, 5: 1004-1007.

Newsham-West R, Nicholson H, Walton M,Milburn P. 2007, Long-term morphology of a healing bone-tendon interface: a histological observation in the sheep model, *J Anat,* **210**, 3: 318-327.

Patte D. 1990, Classification of rotator cuff lesions, *Clin Orthop Relat Res,* 254: 81-86.

Riley GP, Harrall RL, Constant CR, Chard MD, Cawston TE,Hazleman BL. 1994, Tendon degeneration and chronic shoulder pain: changes in the collagen composition of the human rotator cuff tendons in rotator cuff tendinitis, *Ann Rheum Dis,* **53**, 6: 359-366.

Sanchez Marquez JM, Martínez Díez JM, Barco R,Antuña S. 2011, Functional results after arthroscopic repair of massive rotator cuff tears: Influence of the application platelet-rich plasma combined with fibrin, *Rev Esp Cir Ortop Traumatol,* **55**, 282-287.

Schlegel TF, Hawkins RJ, Lewis CW,Turner AS. 2007, An in vivo comparison of the modified Mason-Allen suture technique versus an inclined horizontal mattress suture technique with regard to tendon-to-bone healing: a biomechanical and histologic study in sheep, *J Shoulder Elbow Surg,* **16**, 1: 115-121.

Thomazeau H, Boukobza E, Morcet N, Chaperon J,Langlais F. 1997, Prediction of rotator cuff repair results by magnetic resonance imaging, *Clin Orthop Relat Res,* 344: 275-283.

Thomopoulos S, Genin GM,Galatz LM. 2010, The development and morphogenesis of the tendon-to-bone insertion - What development can teach us about healing, *Journal of Musculoskeletal & Neuronal Interactions,* **10**, 1: 35-45.

Turner AS. 2007, Experiences with sheep surgery: Strengths and as an animal model for shoulder shortcomings, *Journal of Shoulder and Elbow Surgery,* **16**, 5: 158S-163S.

Uggen C, Dines J, McGarry M, Grande D, Lee T,Limpisvasti O. 2010, The effect of recombinant human platelet-derived growth factor BB-coated sutures on rotator cuff healing in a sheep model, *Arthroscopy,* **26**, 11: 1456-1462.

Vavken P, Sadoghi P, Palmer M, Rosso C, Mueller AM, Szoelloesy G,Valderrabano V. 2015, Platelet-Rich Plasma Reduces Retear Rates After Arthroscopic Repair of Small- and Medium-Sized Rotator Cuff Tears but Is Not Cost-Effective, *The American journal of sports medicine,*

Warth RJ, Dornan GJ, James EW, Horan MP,Millett PJ. 2015, Clinical and Structural Outcomes After Arthroscopic Repair of Full-Thickness Rotator Cuff Tears With and Without Platelet-Rich Product Supplementation: A Meta-analysis and Meta-regression, *Arthroscopy,* **31**, 2: 306-320.

Yamaguchi K, Tetro AM, Blam O, Evanoff BA, Teefey SA,Middleton WD. 2001, Natural history of asymptomatic rotator cuff tears: A longitudinal analysis of asymptomatic tears detected sonographically, *Journal of Shoulder and Elbow Surgery,* **10**, 3: 199-203.

Zelzer E, Blitz E, Killian ML,Thomopoulos S. 2014, Tendon-to-bone attachment: from development to maturity, *Birth Defects Res C Embryo Today,* **102**, 1: 101-112.

Zhao J-G, Zhao L, Jiang Y-X, Wang Z-L, Wang J,Zhang P. 2015, Platelet-Rich Plasma in Arthroscopic Rotator Cuff Repair: A Meta-analysis of Randomized Controlled Trials, *Arthroscopy,* **31**, 1: 125-135.

Table 1. Design of the chronic repair study.

Sheep #	Treatment Right shoulder	Treatment Left shoulder	Necropsy
1	ISP tendon initially left intact. 6 weeks later, tendon transected and capped with 5 mm silicon	ISP tendon transected and capped with 5 cm silicon 6 weeks later, tendon was found to be unrepairable	6 week chronicity + 2 weeks
2	ISP tendon initially left intact. 6 weeks later, tendon transected and capped with 5 mm silicon	ISP tendon transected and capped with 5 cm silicon 6 weeks later, tendon was found to be unrepairable	6 week chronicity + 2 weeks
3	ISP tendon transected and capped with 5 cm silicon. 6 weeks later, tendon repaired with 1 suture anchor + CS-PRP	Intact control	6 week chronicity + 2 weeks
4	ISP tendon transected and capped with 5 cm silicon. 6 weeks later, tendon repaired with 1 suture anchor + CS-PRP	Intact control	6 week chronicity + 2 weeks

Table 2. Design of the acute repair study.

Sheep #	Treatment Right shoulder	Treatment Left shoulder	Necropsy
1	Tendon transected and immediately repaired with 4 suture anchors	Intact control	6 weeks
2	Intact control	Tendon transected and immediately repaired with 4 suture anchors	3 months
3	Tendon transected and immediately repaired with 4 suture anchors + CS-PRP	Intact control	6 weeks
4	Intact control	Tendon transected and immediately repaired with 4 suture anchors + CS-PRP	3 months

Figure legends

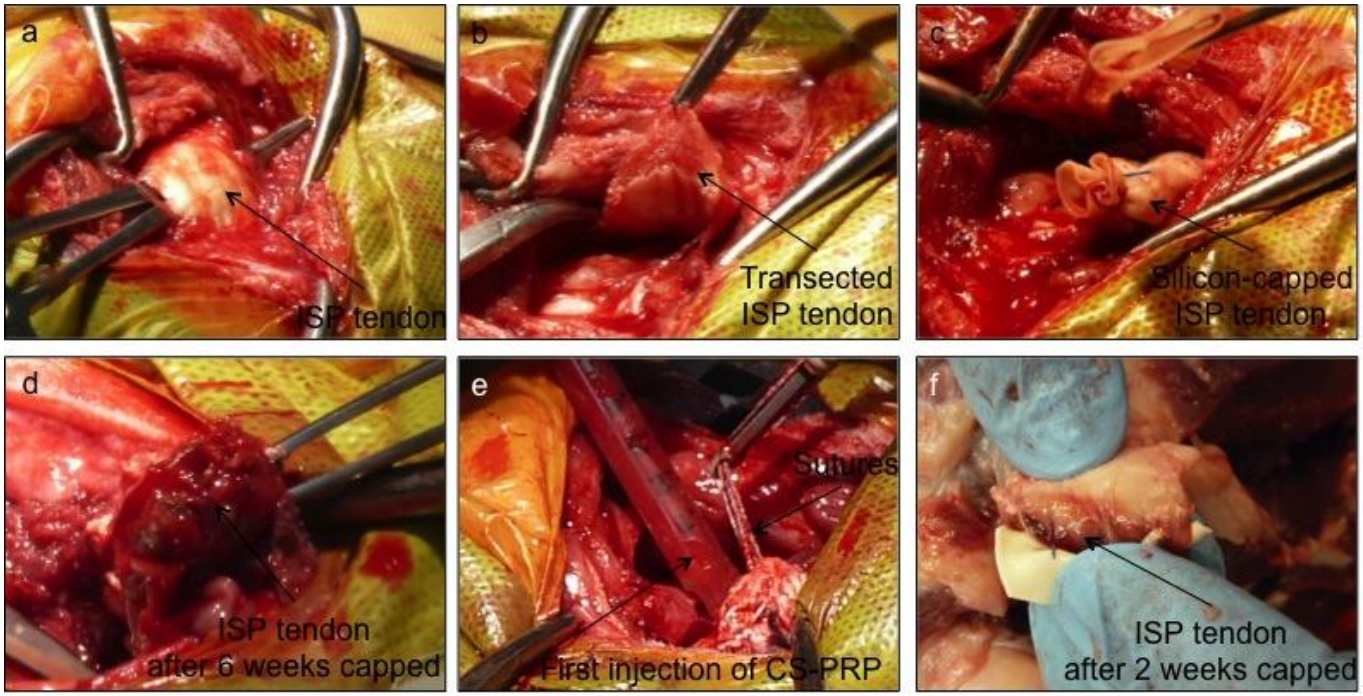

Figure 1. Chronic tear model and repair with CS-PRP. Full-thickness rotator cuff tears were created in the infraspinatus (ISP) tendon of the shoulder close to the enthesis (a, b) and capped with 5 cm length of silicon (c). At 6 weeks after surgery, the tendons were macroscopically abnormal (d) and one tendon was repaired with one suture anchor + CS-PRP. The sutures were pre-placed in a

Mason-Allen pattern and a first injection of 0.5 mL CS-PRP was applied at the debrided bone interface (e). The anchor was inserted to tighten the sutures and an additional 0.5 mL CS-PRP implant was applied on top of tendon at the repaired site and also under the tendon. Macroscopic appearance of an ISP tendon capped for 2 weeks with 5 mm length of silicon (f).

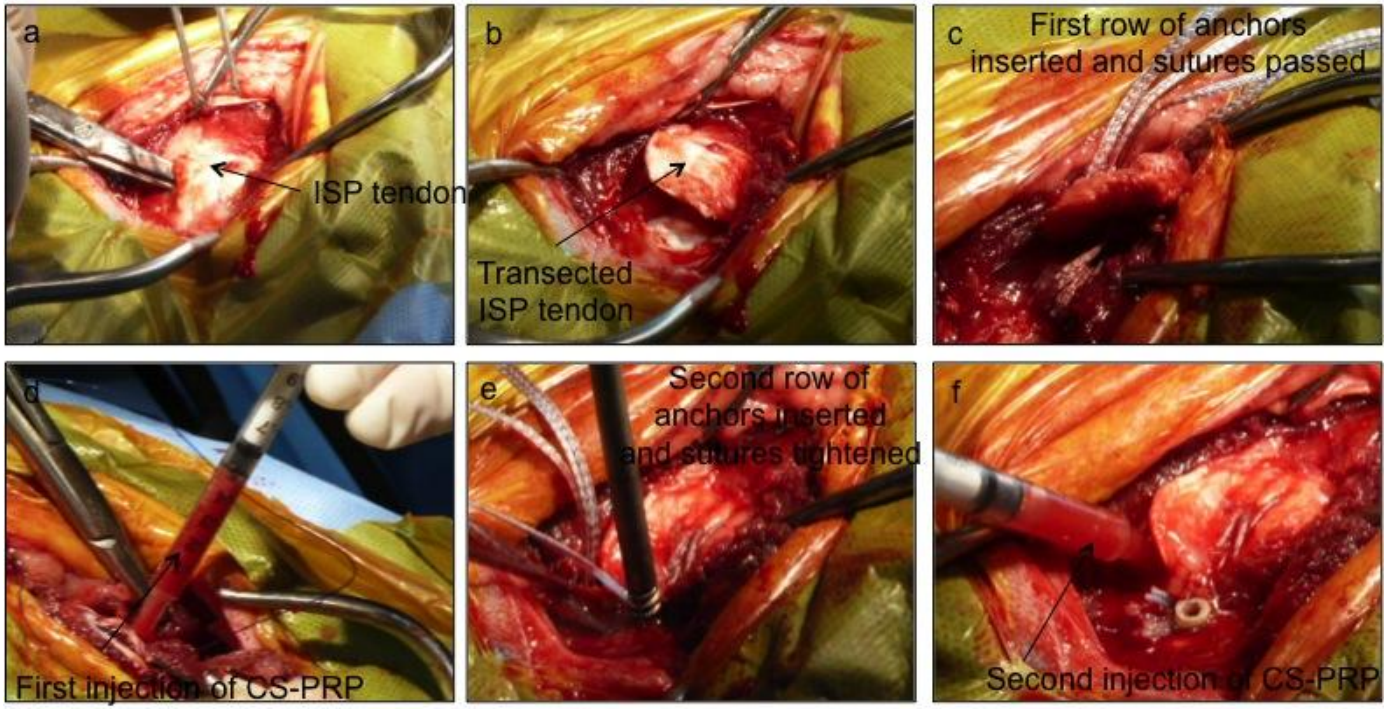

Figure 2. Acute tear model and repair with CS-PRP. Full-thickness rotator cuff tears were created in the infraspinatus (ISP) tendon of the shoulder close to the enthesis (a, b). The tendons were immediately repaired with 4 suture anchors + CS-PRP. The first row of anchors were inserted and the sutures were passed (c) and a first injection of 0.5 mL CS-PRP was applied at the debrided bone interface (d). The second row of anchors were inserted to tighten the sutures (e) and an additional 0.5 mL CS-PRP was applied on top of tendon at the repaired site and also under the tendon (f).

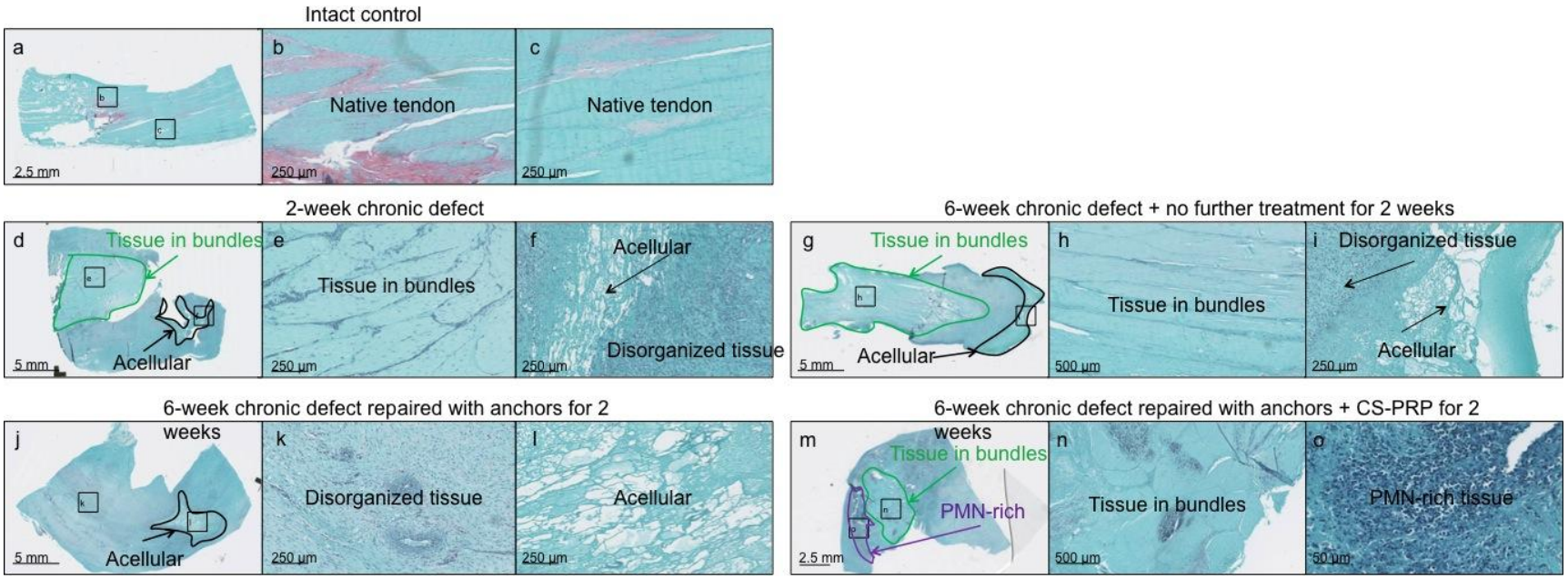

Figure 3. Safranin O/Fast Green stained paraffin sections of the ISP tendons in the chronic repair model. Intact control tendons were organized in bundles, as expected (a to c). Bundle organization was still apparent in areas of untreated tendons at chronic stage, while other areas were disorganized, hypercellular and vascularized or hypocellular (d to i). The tendon of the shoulder treated for 2 weeks with suture anchors was mostly disorganized, hypercellular and vascularized , with a small hypocellular area (j to l). The tendon of the shoulder treated with suture anchors + CS-PRP was mostly disorganized, hypercellular and vascularized , with a small area organized in bundles and another area rich in polymorphonuclear cells (m to o).

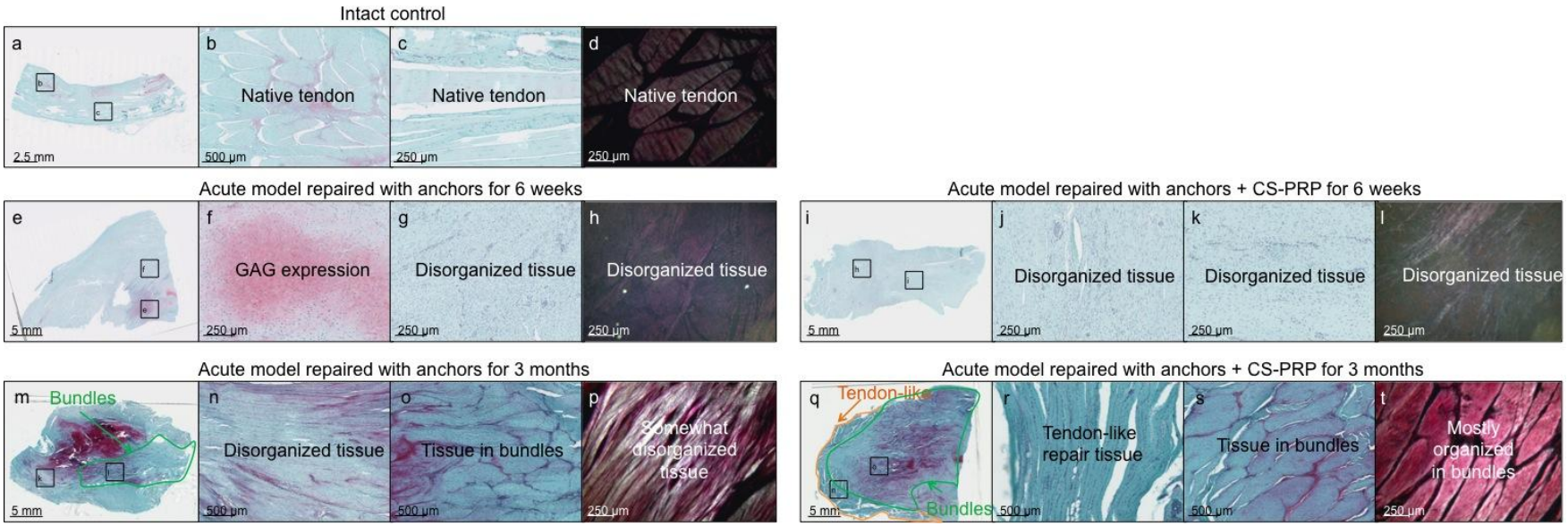

Figure 4. Safranin O/Fast Green-stained paraffin sections and polarized light microscopy (d, h, l, p & t) images of the ISP tendons in the acute repair model. Intact control tendons were organized in bundles, as expected (a to d). At 6 weeks post-surgery, the tendons were mostly composed of a disorganized and vascular fibrous repair tissue in both groups (e to l). Chondrogenesis and GAG expression were apparent in the anchors only group at 6 weeks (e&f). At 3 months post-surgery, the tendon in the anchors only group was mostly disorganized, expressed high levels of GAG, and had a small area organized in bundles (m to p). In contrast, the tendon in the anchors + CS-PRP group was mostly organized in bundles with a smaller area of tendon-like repair tissue (m to t).

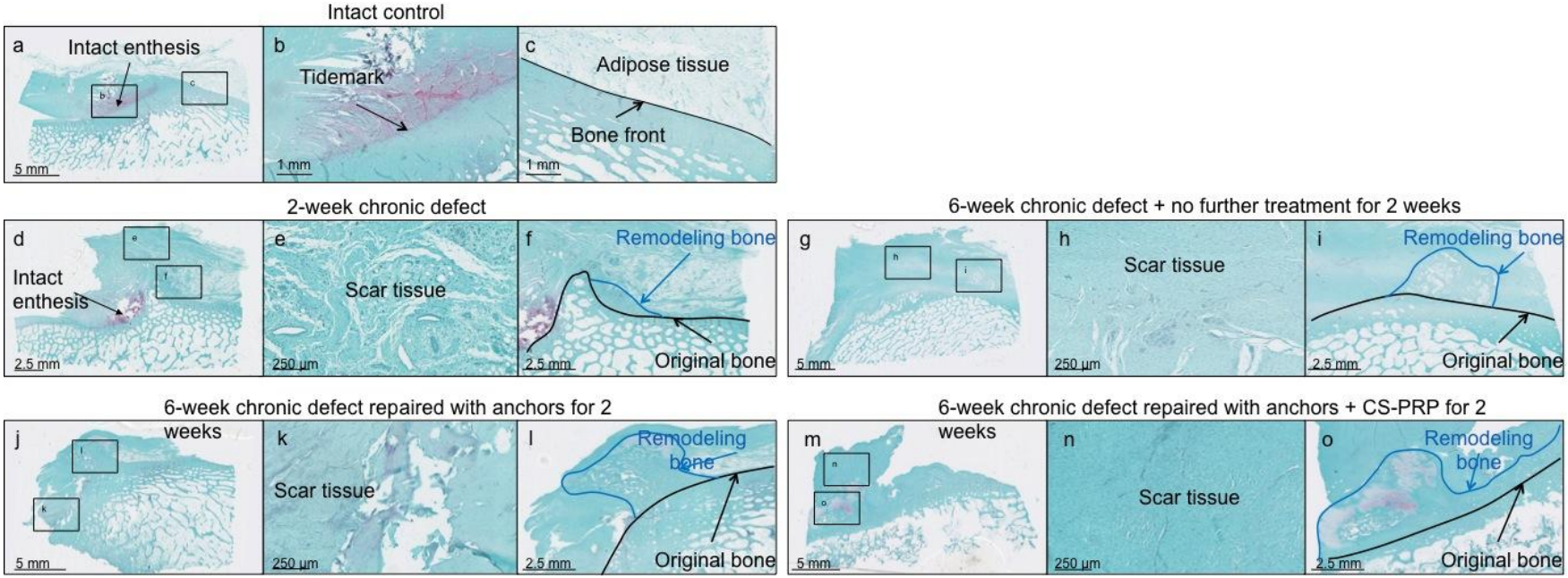

Figure 5. Safranin O/Fast Green stained paraffin sections of the ISP tendon entheses in the chronic repair model. Intact controls had normal entheses consisting of 1) unmineralized fibrocartilage, 2) tidemark, 3) mineralized fibrocartilage and 4) bone, as expected (a to c). Normal enthesis structural organization was still apparent 2 weeks after defect creation (d), but not at longer time points or after repair (g, j & m). Scar tissue was growing above the entheses in the untreated chronic defects (d&g), suggesting that some spontaneous repair can occur even without any treatment in this model. Integration of the scar tissue with the underlying bone was achieved through bone remodeling and ingrowth into the scar tissue (f, i, l & o). Treatment with anchors + CS-PRP increased the area of remodeling bone (compare o to l).

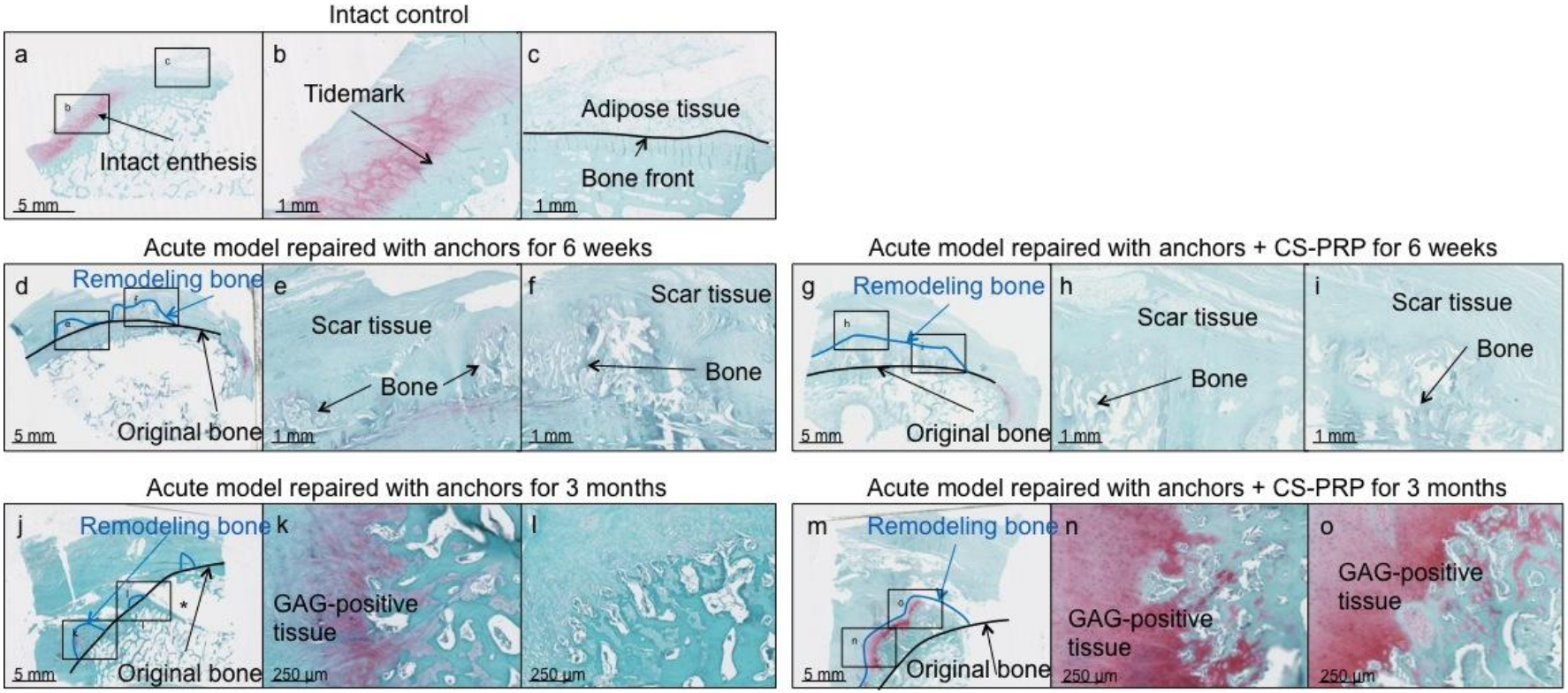

Figure 6. Safranin O/Fast Green stained paraffin sections of the ISP tendon entheses in the acute repair model. Intact controls had normal entheses consisting of 1) unmineralized fibrocartilage, 2) tidemark, 3) mineralized fibrocartilage and 4) bone, as expected (a to c). Scar tissue was growing superior to the entheses from 6 weeks (d to i) to 3 months (j to o) post-surgery. Integration of the scar tissue with the underlying bone was achieved through bone remodeling and ingrowth into the scar tissue (d to o). This was more

apparent in the anchors + CS-PRP group (compare g&m to d&j). Expression of GAG was abundant at the insertion site in the anchors + CS-PRP group at 3 months (m to o). The site of anchor insertion was apparent in some sections (* in panel j).

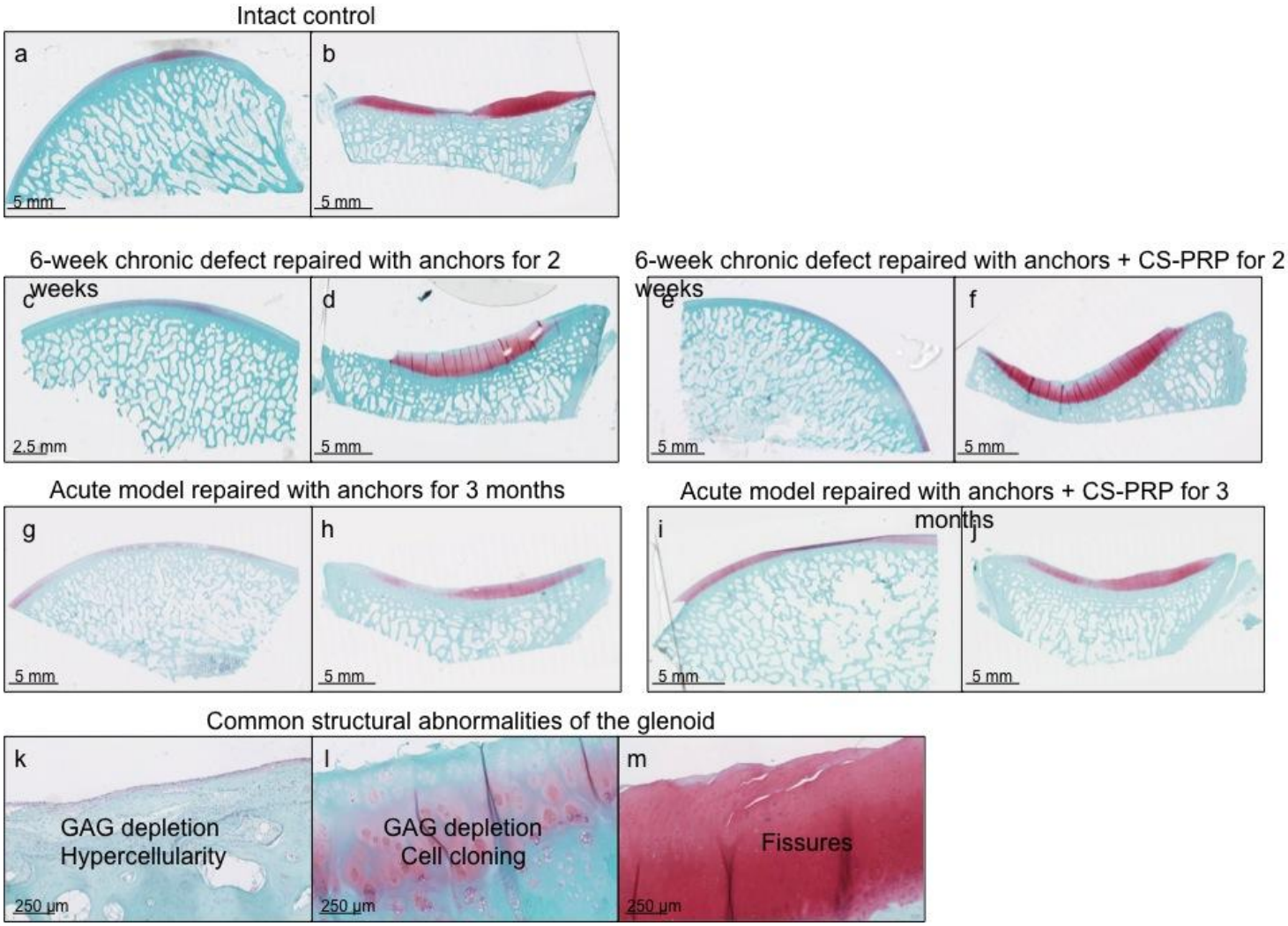

Figure 7. Safranin O/Fast Green stained sections of humeral head and glenoid articular surfaces from intact controls (a&b), from the chronic defect model (c to f) and from the acute defect model (g to j). The humeral articular surfaces were all structurally normal but

showed signs of GAG depletion (a, c, e, g & i). Mild structural abnormalities were observed at the center of some glenoid articular surfaces, including GAG depletion, hypercellularity, cell cloning and fissures (k to m). These were apparent in all treatment groups as well as the intact controls.

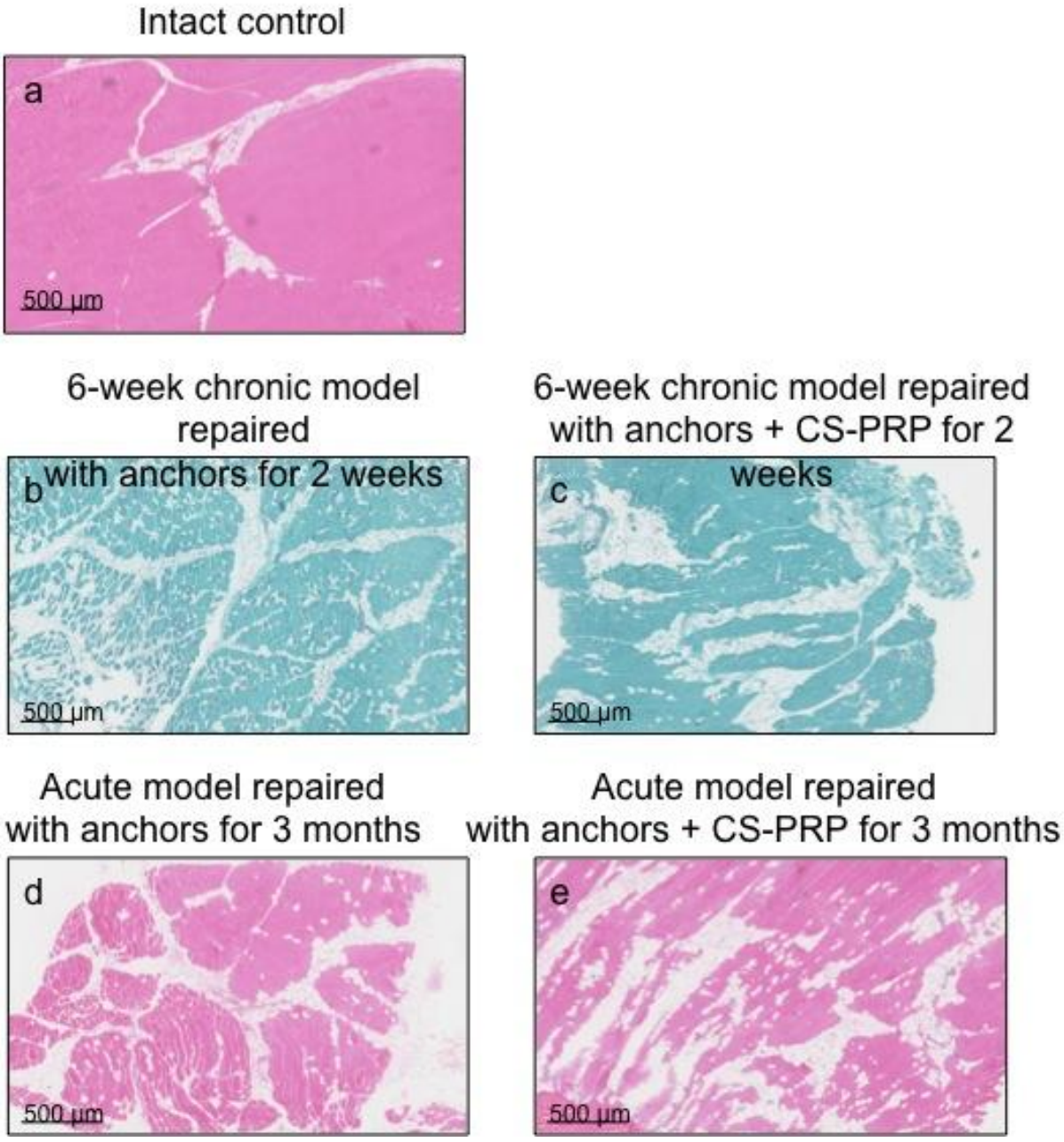

Figure 8. Hematoxylin and Eosin (a, d & e) and Safranin O/Fast Green (b & c) stained paraffin sections of muscle biopsies from intact control (a), from the chronic defect model (b & c) and from the acute defect model (d & f). Fatty infiltration was not prevented by any treatment.

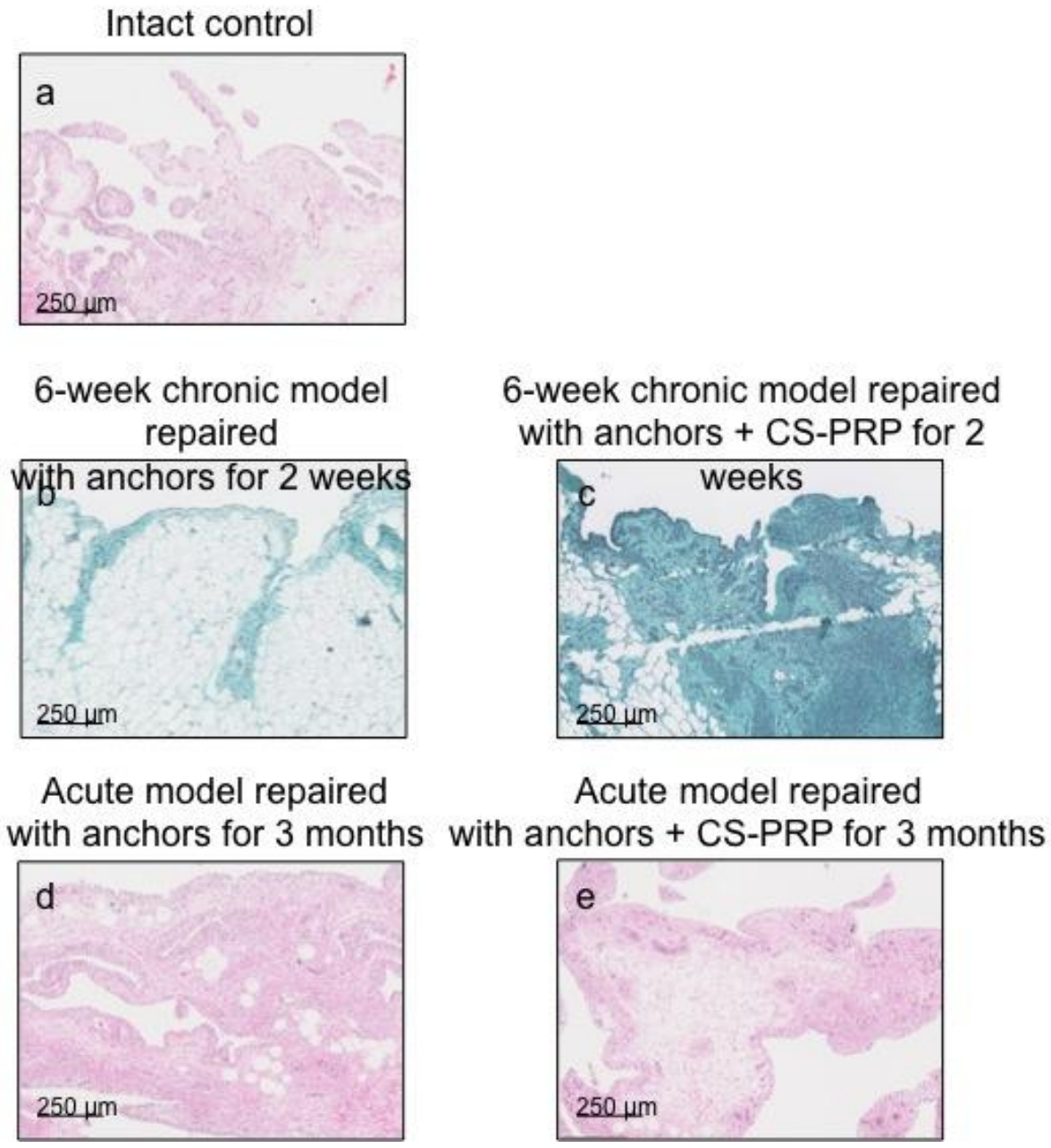

Figure 9. Hematoxylin and Eosin (a, d & e) and Safranin O/Fast Green (b & c) stained paraffin sections of synovial biopsies from intact control (a), from the chronic defect model (b & c) and from the acute defect model (d & f). There was mild synovitis and increased cell infiltration in the chronic model treated with anchors + CS-PRP for 2 weeks (c).